

## Supporting Information

# An amyloid-like proteinaceous adsorbent for uranium extraction from aqueous medium

*Qingmin Yang,<sup>a</sup> Jian Zhao,<sup>\*b</sup> Arif Muhammad,<sup>b</sup> Rongrong Qin,<sup>b</sup> Juanhua Tian,<sup>c</sup> Ling Li,<sup>b</sup>*

*Qianhui Zhang,<sup>b</sup> Lixin Chen<sup>\*a</sup> and Peng Yang<sup>\*b</sup>*

<sup>a</sup>School of Chemistry and Chemical Engineering, Northwestern Polytechnical University,  
Xi'an 710072, China. E-mail: [lixin@nwpu.edu.cn](mailto:lixin@nwpu.edu.cn)

<sup>b</sup>Key Laboratory of Applied Surface and Colloid Chemistry, Ministry of Education, School of  
Chemistry and Chemical Engineering, Shaanxi Normal University, Xi'an 710119, China.  
E-mail: [zhaojian@snnu.edu.cn](mailto:zhaojian@snnu.edu.cn), [yangpeng@snnu.edu.cn](mailto:yangpeng@snnu.edu.cn)

<sup>c</sup>Department of Urology, The Second Affiliated Hospital of Xi'an Jiaotong University,  
West Five Road, No. 157, Xi'an 710004, China.

## **1. Experimental Section**

### **1.1. Materials**

Lysozyme, Thioflavin-T (ThT) and 8-anilino-1-naphthalenesulfonic (ANS) were purchased from Sigma-Aldrich. Tris (2-carboxyethyl) phosphine hydrochloride (TCEP) was purchased from TCI. *N*-(1-pyrenyl)maleimide (NPM) was purchased from Shanghai Yuanye Science and Technology Co., Ltd. Hydroxypropyl- $\beta$ -Cyclodextrin and *N,N'*-Disuccinimidyl Carbonate were purchased from Aladdin. Dulbecco's modified eagle medium (DMEM) was purchased from Hyclone. Sodium hydroxide (NaOH), hydrochloric acid (36%~38% HCl) and nitric acid (68% HNO<sub>3</sub>) were purchased from Sinopharm Chemical. All Inductively Coupled Plasma Mass Spectrometry (ICP-MS) standard solutions (100 ppm of Co, Fe, V, Cd, Pb, As, etc. in 2 M HNO<sub>3</sub>, 1000 ppm of U in HCl) were purchased from Aladdin. Ultrapure water was used in all experiments and was supplied by Milli-Q Advantage A10 (Millipore, USA).

### **1.2. Characterization**

MALDI-TOF analysis of lysozyme, hydroxypropyl- $\beta$ -Cyclodextrin and lysozyme- $\beta$ -Cyclodextrin was carried out on a Bruker MALDI-TOF Ultraflex II machine. Far-UV circular dichroism (CD) spectrum was collected by using Chirascan spectrophotometer (Applied Photophysics Ltd, England). The fluorescence spectrum was collected by an F-7000 fluorescence spectrophotometer (Hitachi). Surface zeta potential measurement was performed by SurPASS electrokinetic analyzer (Anton Paar GmbH, Austria). X-ray photoelectron spectroscopy (XPS) was performed with AXIS Ultra from Kratos Analytical Ltd. (Japan), and the binding energies were calibrated by setting the C1s peak at 284.6 eV. Fourier transform infrared (FTIR) spectra were recorded on a Tensor 27 (Bruck). Laser scanning confocal microscopy (LSCM) observation was conducted on FV1200 (Olympus). Scanning electron microscopy (SEM) analyses were carried out using a field emission scanning electron microscope (FE-SEM) (SU8220, Hitachi) at an acceleration voltage of 5 kV. Cytotoxicity data is tested using a microplate reader (Multiskan GO, Thermo Scientific). The Brunauer–Emmett–Teller (BET) surface area was obtained via nitrogen absorption-desorption on a surface aperture adsorption instrument (ASAP2020, Micromeritics, USA). Inductively coupled plasma mass spectrometry (ICP-MS, aurora M90, Bruker, USA) was utilized to measure the concentration of U and other metals. The samples were filtered by 0.22  $\mu$ m membrane filter, diluted by ultrapure 1% HNO<sub>3</sub>, and the content of metal ions was analyzed by comparison with the standard solutions.

### 1.3. Synthesis of Lysozyme- $\beta$ -CD

375 mg hydroxypropyl- $\beta$ -cyclodextrin (HP- $\beta$ -CD, Mw=1500) and 200  $\mu$ L triethylamine (TEA) were added into 20 mL dimethyl sulfoxide (DMSO) in sequence. When HP- $\beta$ -CD dissolved completely, 192 mg N,N'-disuccinimidyl carbonate (DSC) was added into the solution and the reaction was taken at room temperature for 8 hours. The reacted solution was then purified using a rotary evaporator at 70 °C for more than 30 minutes to remove triethylamine to obtain N-succinimidyl-activated  $\beta$ -Cyclodextrin (NHS- $\beta$ -CD) DMSO solution. 1191 mg lysozyme/20 mL DMSO solution was added into the above obtained NHS- $\beta$ -CD/DMSO solution, after reacted at room temperature for 8 hours, the solution was dialyzed by the dialysis bag with a molecular weight of 3500 for 72 hours to remove DMSO and unreacted reactants. Finally, white solid lysozyme- $\beta$ -CD conjugates powder was obtained after freeze-drying (1020 mg, 85.64%).

### 1.4. Lysozyme- $\beta$ -CD molecular weight test

Matrix-assisted laser desorption ionization time-of-flight mass spectrometry (MALDI-TOF) was used to characterize the molecular weight. Lysozyme (2 mg/mL, 1.5  $\mu$ L) and Lysozyme- $\beta$ -CD solution (2 mg/mL, 1.5  $\mu$ L) were mixed with an equal volume of  $\alpha$ -Cyano-4-Hydroxycinnamic acid solution (10 mg/mL, 1.5  $\mu$ L), and then dropped on the test target plate.

### 1.5. Lysozyme- $\beta$ -CD activity test

The activity test was carried out according to the standard test scheme. Lysozyme- $\beta$ -CD (2 mg/mL), lysozyme (2 mg/mL) and  $\beta$ -CD (2 mg/mL) aqueous solutions were put in water bath at 37 °C for 5 min, and then the bacterial solution (0.25 mg/mL) was mixed with the above three solutions at equal volume ( $V/V=1/1$ ). Finally, the transmittance of samples was measured by UV spectrophotometer at 0 min and 2 min, respectively.

### 1.6. Far-UV CD assay

The concentration of Lysozyme and Lysozyme- $\beta$ -CD was set at 0.2 mg/mL. PTL- $\beta$ -CD was prepared by Lysozyme- $\beta$ -CD (0.2 mg/mL) and TCEP (5 mM, pH 7.0). Far-UV CD spectra recorded from 190 nm to 260 nm with a 2.0 nm bandwidth were then collected under constant nitrogen flush at 25 °C.

### 1.7. ThT staining

The PTL- $\beta$ -CD aggregates were obtained on the glass interface, dried and stained in a ThT aqueous solution (1 mM) for 60 min in the dark. The fluorescence microscope photograph was taken by LSCM after washing by deionized water.

100  $\mu$ L of 1 mM ThT and 1500  $\mu$ L lysozyme- $\beta$ -CD (2 mg/mL) were added into a quartz cell, followed by the addition of 1500  $\mu$ L TCEP (50 mM). The sample was then measured by fluorescence spectrophotometer with excitation wavelength 440 nm and emission wavelength 484 nm, respectively. The bandwidths of excitation and emission slits were set as 5 nm.

### **1.8. ANS staining**

100  $\mu$ L of 1 mM ANS and 1500  $\mu$ L lysozyme- $\beta$ -CD (2 mg/mL) were added into a quartz cell, followed by the addition of 1500  $\mu$ L TCEP (50 mM). The sample was then measured by fluorescence spectrophotometer with excitation wavelength 398 nm and emission wavelength 470 nm, respectively. The bandwidths of excitation and emission slits were set as 2.5 nm.

### **1.9. NPM staining**

100  $\mu$ L of 1 mM NPM in DMF and 1500  $\mu$ L of 50 mM TCEP were added into a quartz cell, followed by the addition of 1500  $\mu$ L lysozyme- $\beta$ -CD (2 mg/mL). The sample was then measured by fluorescence spectrophotometer with excitation wavelength 330 nm and emission wavelength 380 nm, respectively. The bandwidths of excitation and emission slits were set as 5 nm.

### **1.10. Preparation of PTL- $\beta$ -CD aggregates**

Lysozyme- $\beta$ -CD solution (10 mg/mL) and TCEP buffer (50 mM pH 7.0 ) were mixed at equal volume ratio ( $V/V=1/1$ ) and reacted for 2 h at room temperature. After the reaction, the white PTL- $\beta$ -CD aggregate solid powder was obtained by centrifugation, washing, and freeze-drying.

### **1.11. Preparation cost of PTL- $\beta$ -CD aggregates**

Preparation of 1 g PTL- $\beta$ -CD requires 1.17 g lysozyme (\$0.123), 0.37 g  $\beta$ -CD (\$0.067), 0.225 g DSC (\$0.0512), TCEP 0.286 g (\$0.18), the total cost is \$0.42.

## **2. Adsorption performance of uranium ions**

### **2.1. Adsorption of uranium ions by PTL- $\beta$ -CD aggregates**

Dissolved sea salt in water to obtain simulated seawater referring to the instructions for use (33 g sea salt is dissolved in 1 L of water). Then the uranium ion standard solution was diluted with simulated seawater to obtain uranium ion solutions of different concentrations. The prepared 5 mg PTL- $\beta$ -CD aggregates were added into 10 mL uranium ion solution with a certain concentration. After adsorption for a certain time, the residual uranium ion concentration in the solution was determined by ICP-MS. 0.1 M HCl or 0.1 M Na<sub>2</sub>CO<sub>3</sub> was used to adjust the initial uranium ion solutions pH.

## 2.2. PTL-β-CD aggregates selective adsorption of uranium ions

Mixed metal ions solutions with each initial concentration of 1 ppm were prepared by diluting the standard mixed metal ions solution by 10 mL of 1% HNO<sub>3</sub> to obtain a solution with an initial concentration of 1 ppm.

The effect of anions on uranium ion adsorption was carried out in 10 mL 1 ppm uranium ion solution containing 0.01 M Na<sub>2</sub>CO<sub>3</sub>, 0.01 M HCl, 0.01 M HNO<sub>3</sub> or 0.01 M H<sub>2</sub>SO<sub>4</sub>.

## 2.3. Adsorption-desorption experiment of uranium ion

In order to recycle the PTL-β-CD aggregates, uranium ion was extracted from the metal ion loaded PTL-β-CD aggregates by the eluent solution of 1 M HNO<sub>3</sub>, and then the uranium ion concentration in the eluent solution was measured by ICP-MS. The adsorption experiment was performed again on the desorbed PTL-β-CD aggregates.

## 2.4. Cytotoxicity test of the PTL-β-CD aggregates

First, the PTL-β-CD aggregates were formed at the bottom of the 96-well plate. 100 μL of complete Dulbecco's medium containing cells was added into the wells with PTL-β-CD and blank wells, respectively. The plate was then incubated in a cell incubator at 37 °C for 24 h. Microscope was used to check the attachment of the cells. The culture medium was replaced by 200 μL fresh complete medium every 24 hours. At 24 h, 48 h, and 72 h, the supernatant was removed by a pipette and 90 μL fresh medium and 10 μL MTT were added, and the plate was further incubated for 4 hours. The supernatant was then removed and 110 μL DMSO was added following by shaking for 5 minutes, and the absorption value at 490 nm was measured by microplate reader.

## 2.5. Adsorption kinetics

The adsorption ratio ( $R_A$ ) was calculated by the difference of metal ion concentration before and after adsorption (see equation (1)).

$$R_A = \frac{c_0 - c_e}{c_0} \times 100\% \quad (1)$$

In the formula,  $c_0$  and  $c_e$  represent the initial and equilibrium uranium ions concentrations (ppm), respectively.

The adsorption kinetics of uranium ions on the PTL-β-CD aggregate was analyzed via using the pseudo-first-order and pseudo-second-order kinetic models to match the experimental data, which is expressed respectively as:

$$\ln(q_e - q_t) = \ln q_e - k_1 t \quad (2)$$

$$t/q_t = 1/(k_2 \cdot q_e^2) + t/q_e \quad (3)$$

In the formula,  $q_t$  and  $q_e$  (mg/g) are the amounts of metal ions adsorbed per unit mass of the adsorbent at time  $t$  and at equilibrium,  $k_1$  ( $\text{h}^{-1}$ ) is the first order rate constant of adsorption,  $k_2$  ( $\text{g mg}^{-1} \text{h}^{-1}$ ) is the rate constant of adsorption equilibrium in the second order reaction. The relative values calculated from the two models were shown in **Table S1**.

## 2.6. Adsorption isotherm

The adsorption experiment was carried out in 10 mL uranium ion solution. Seawater was used to dilute 1000 ppm uranium ion aqueous solution, and the final uranium ions concentration range is 1 to 20 ppm. The PTL- $\beta$ -CD aggregate was suspended in uranium ion solution. Adsorption experiments were then performed at 288, 298 and 310 K for different hours. After adsorption equilibrium, ICP-MS was used to analyze the uranium ion concentration. The adsorption capacity ( $q_e$ ) is calculated according to formula (4).

$$q_e = \frac{V(C_0 - C_e)}{m} \quad (4)$$

In the formula,  $c_0$  and  $c_e$  represent the initial and equilibrium uranium ion concentrations (ppm), respectively.  $V$  is the volume of uranium ion solution (L), and  $m$  is the dosage of the PTL- $\beta$ -CD aggregate (g).

## 2.7. Langmuir and Freundlich isotherm

In this research, the equilibrium adsorption data was analyzed according to the widely used Langmuir isotherm (5) and Freundlich isotherm (6).

$$c_e/q_e = c_e/q_m + 1/(q_m \cdot k_L) \quad (5)$$

$$q_e = k_F c_e^{1/n} \quad (6)$$

In the formulas,  $c_e$  is the equilibrium concentration of metal ions remained in the solution (ppm);  $q_e$  is the amount of metal ions adsorbed on per unit of mass solid adsorbent after equilibrium (mg/g);  $q_m$ , the maximum adsorption capacity that is the amount of adsorbate at complete monolayer coverage (mg/g), and  $k_L$  (L/mg) is a constant that is related to the heat of adsorption.  $k_F$  and  $n$  are Freundlich constants related to adsorption capacity and intensity of adsorption. The relative values worked out from the two models were shown in **Table S2**.

## 2.8. Thermodynamic analysis

The thermodynamic parameters such as Gibbs free energy change ( $\Delta G^0$ ), enthalpy ( $\Delta H^0$ ) and entropy ( $\Delta S^0$ ) were calculated using the following equations:

$$\Delta G^0 = -RT \ln K_C \quad (7)$$

$$\Delta G^0 = \Delta H^0 - T\Delta S^0 \quad (8)$$

where  $K_C$  is the distribution coefficient for adsorption and is determined as:

$$K_C = c_a/c_e \quad (9)$$

where  $c_a$  is the equilibrium uranium ion concentration on the adsorbent (mg/L) and  $c_e$  is the equilibrium uranium ion concentration in solution (mg/L). The thermodynamic parameters were shown in **Table S3**.

Supporting Figures:

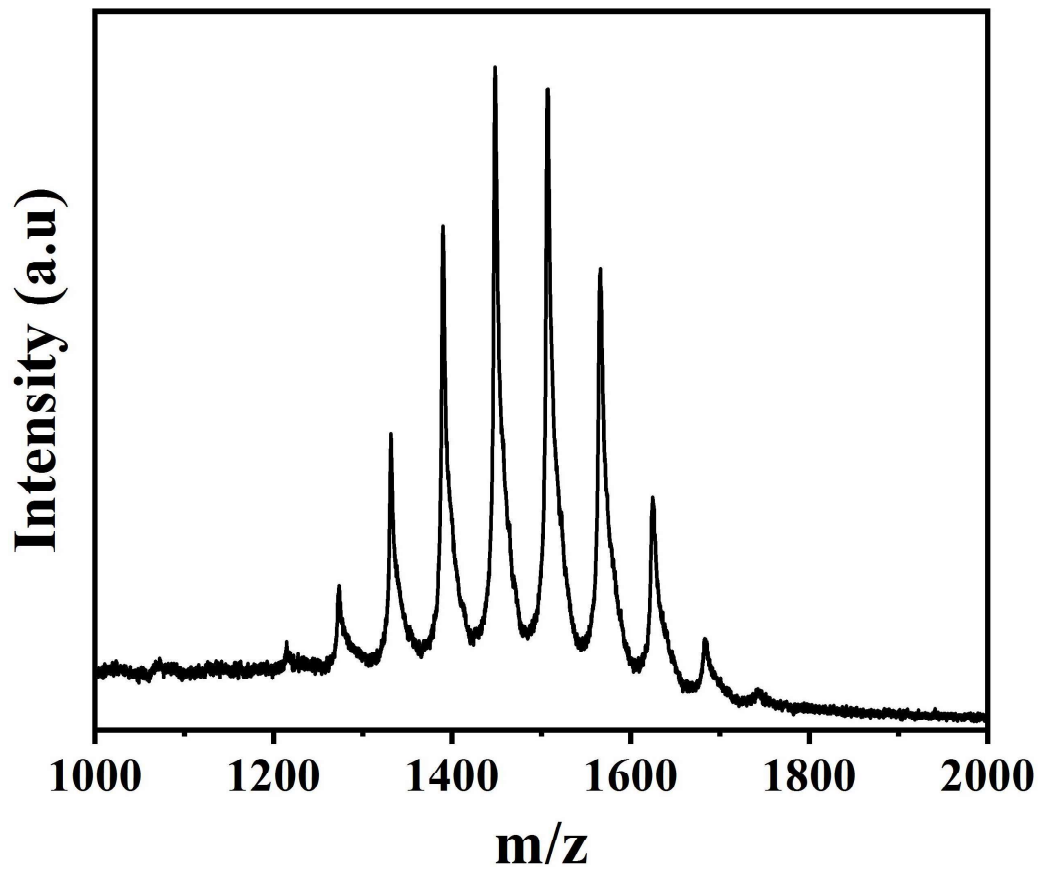
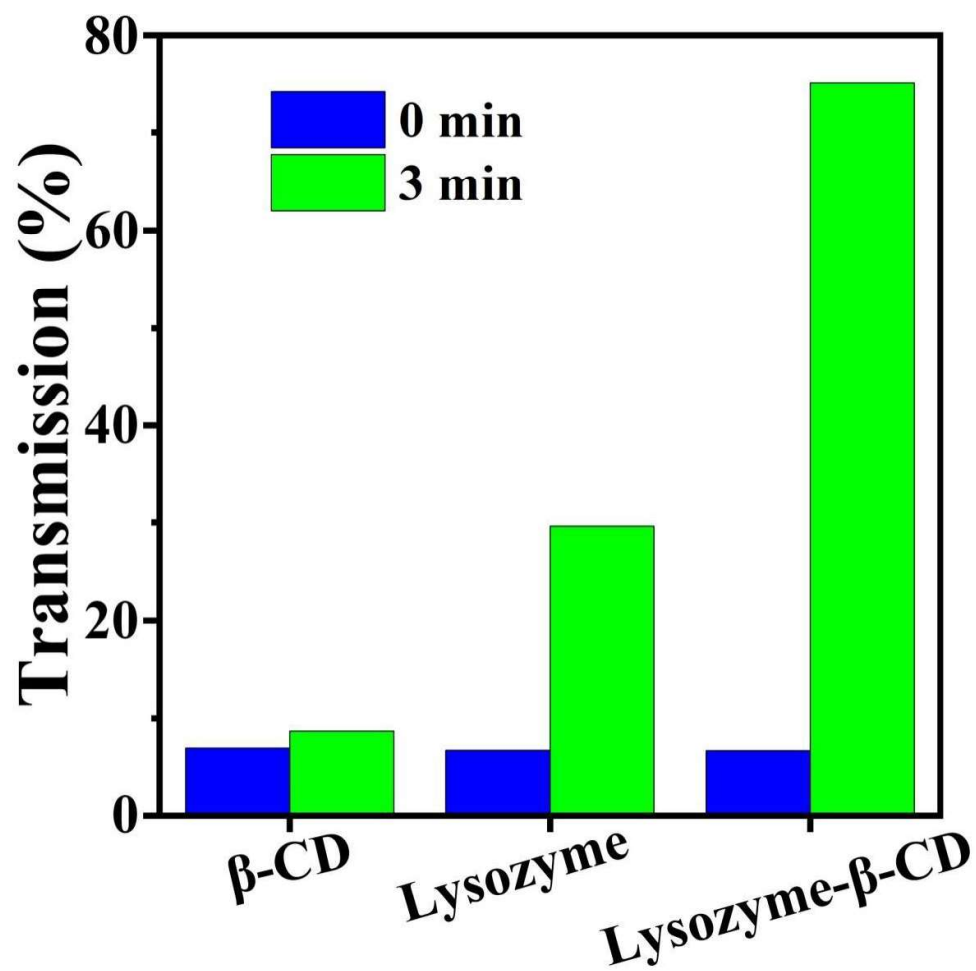
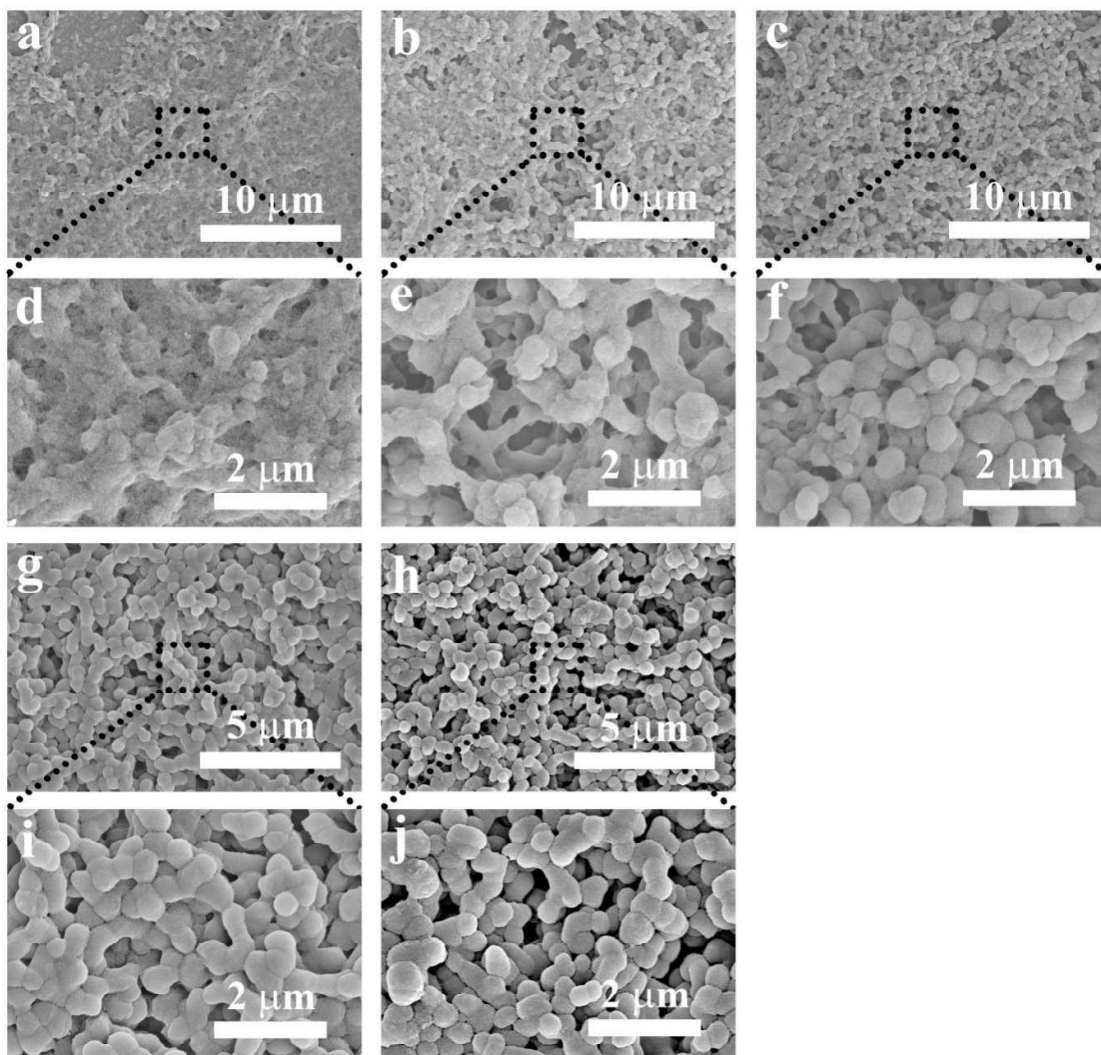


Figure S1. MALDI-TOF spectra of hydroxypropyl- $\beta$ -Cyclodextrin.





**Figure S2.** The activity of  $\beta$ -CD, lysozyme, and lysozyme- $\beta$ -CD were evaluated by spectrophotometry.



**Figure S3.** SEM images of the PTL- $\beta$ -CD prepared with the pH of TCEP buffer at 4.0 (**a&d**), 5.0 (**b&e**), 6.0 (**c&f**), 7.0 (**g&i**), 8.0 (**h&j**), respectively. In these cases, the concentration of lysozyme- $\beta$ -CD was 10 mg/mL, the concentration of TCEP was 50 mM, reaction time was 12 hours.

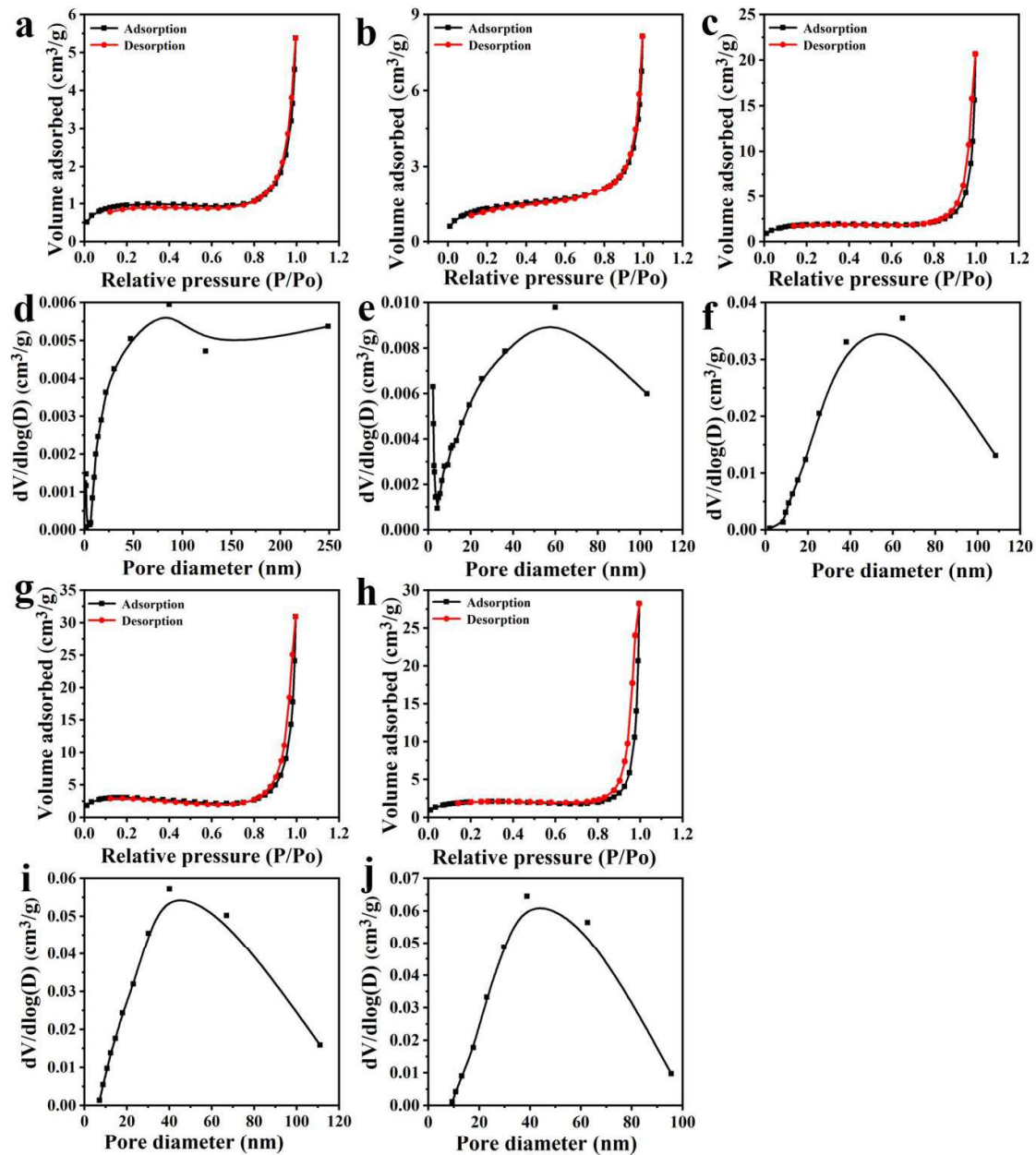


**Figure S4.** The nitrogen adsorption-desorption isotherms and corresponding pore size distributions for the PTL- $\beta$ -CD prepared with the pH of TCEP buffer at 4.0 (a&d), 5.0 (b&e), 6.0 (c&f), 7.0 (g&i), 8.0 (h&j), respectively. In these cases, the concentration of lysozyme- $\beta$ -CD was 10 mg/mL, the concentration of TCEP was 50 mM, reaction time was 12 hours.

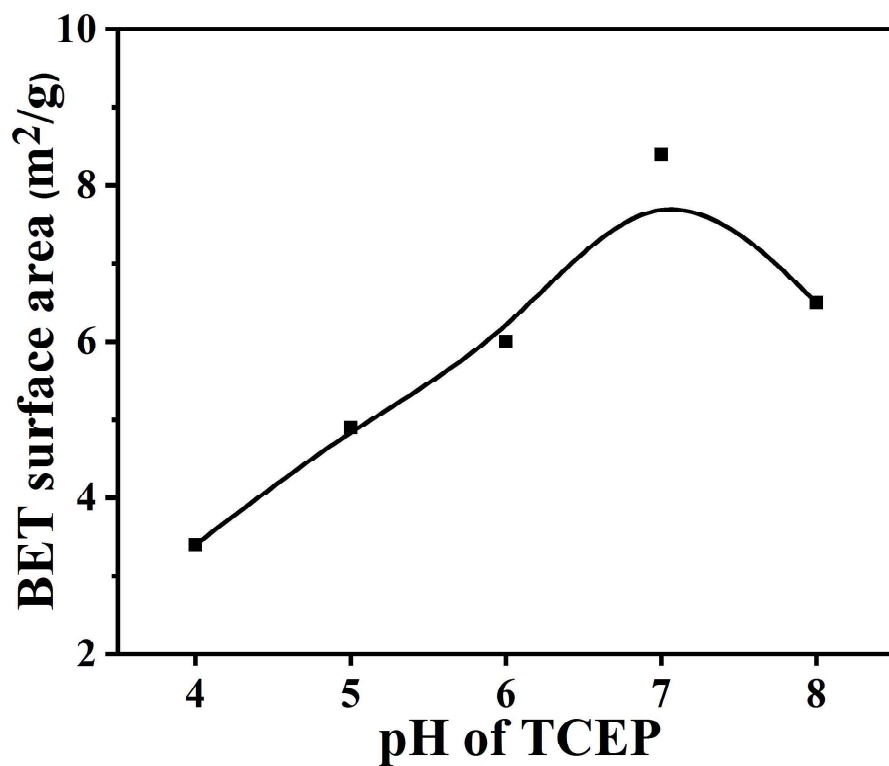


**Figure S5.** The BET surface area of PTL- $\beta$ -CD prepared with the pH of TCEP buffer 4.0, 5.0, 6.0, 7.0 and 8.0, respectively. In these cases, the concentration of lysozyme- $\beta$ -CD was 10 mg/mL, the concentration of TCEP was 50 mM, reaction time was 12 hours.

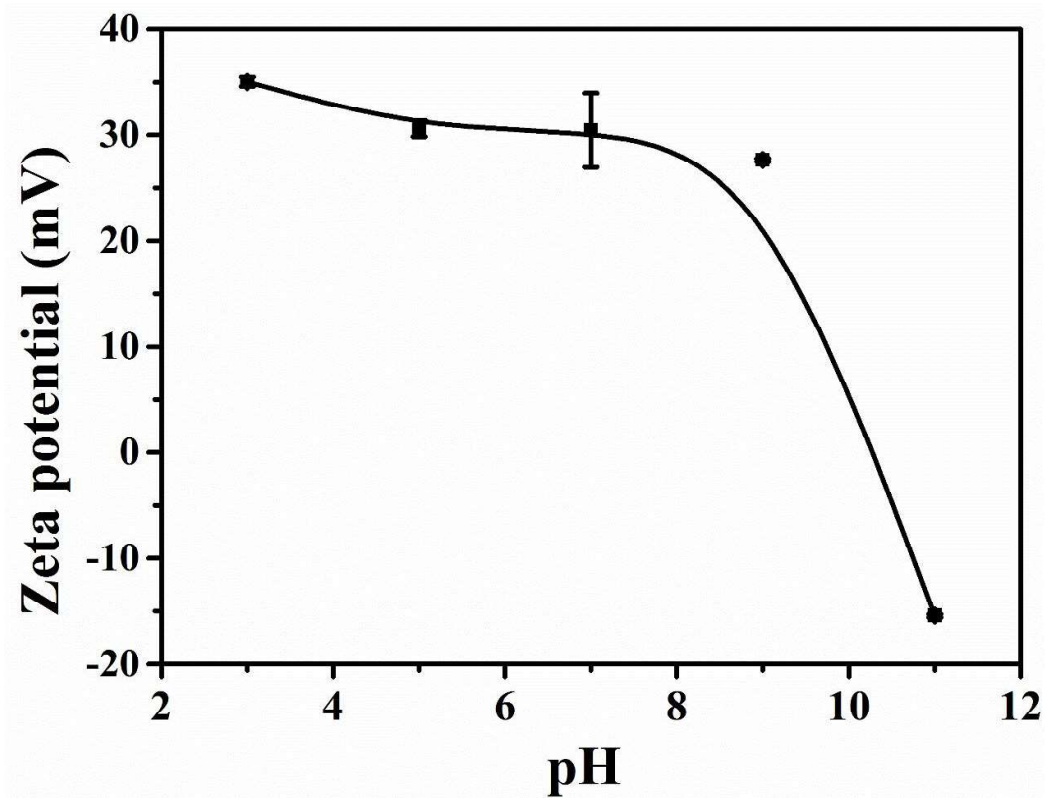


**Figure S6.** The zeta potential of the Lysozyme- $\beta$ -CD in solution with different pH.

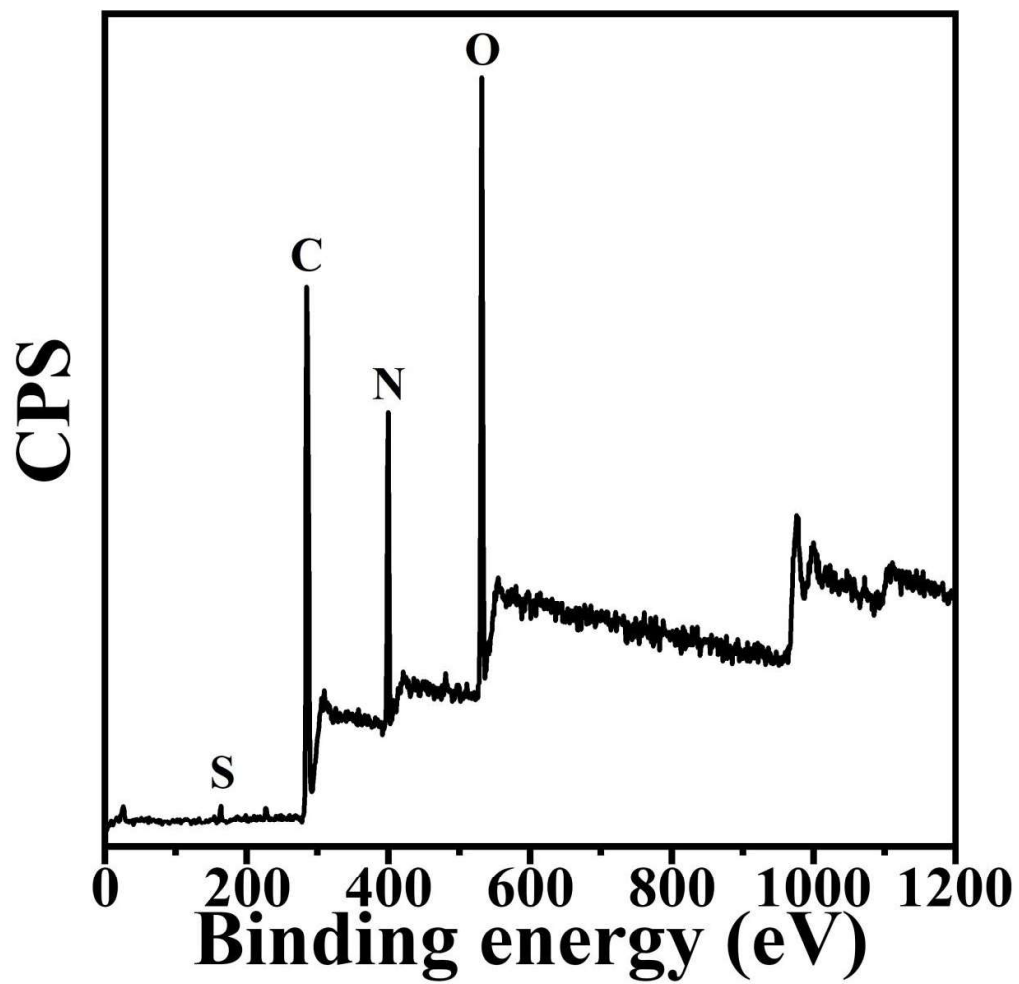


**Figure S7.** XPS spectrum of the PTL- $\beta$ -CD.

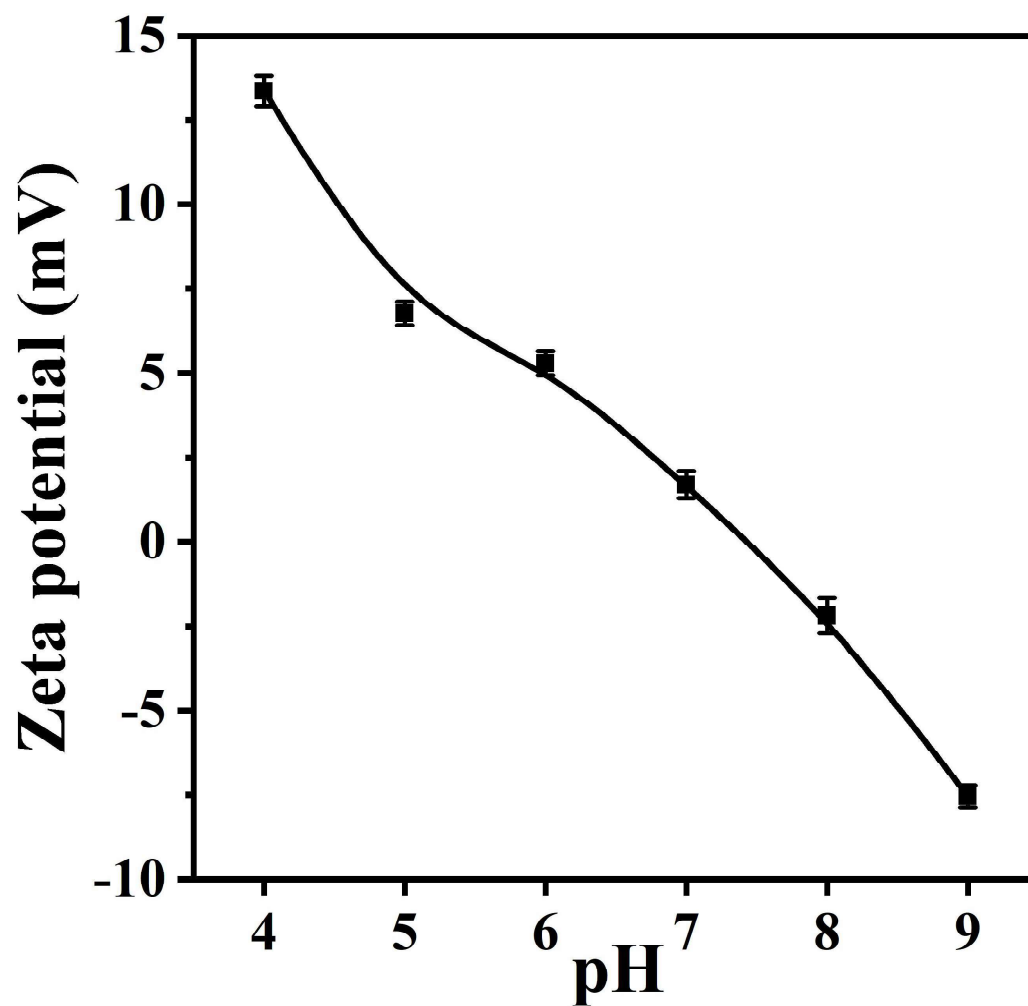


**Figure S8.** The zeta potential of the PTL- $\beta$ -CD aggregates in solution with different pH.

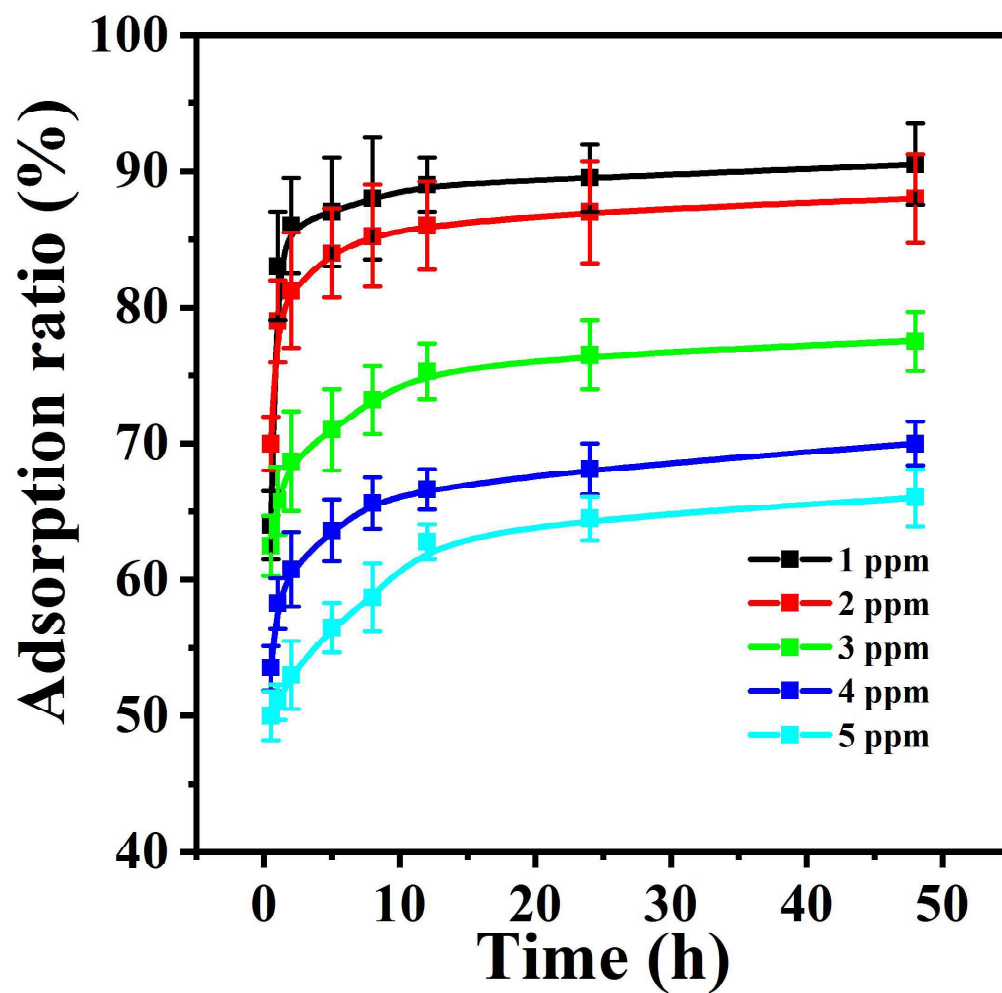


**Figure S9.** At different initial concentration of uranium ions, time-dependent adsorption ratio of the PTL- $\beta$ -CD in uranium ions aqueous solutions with different initial concentration.



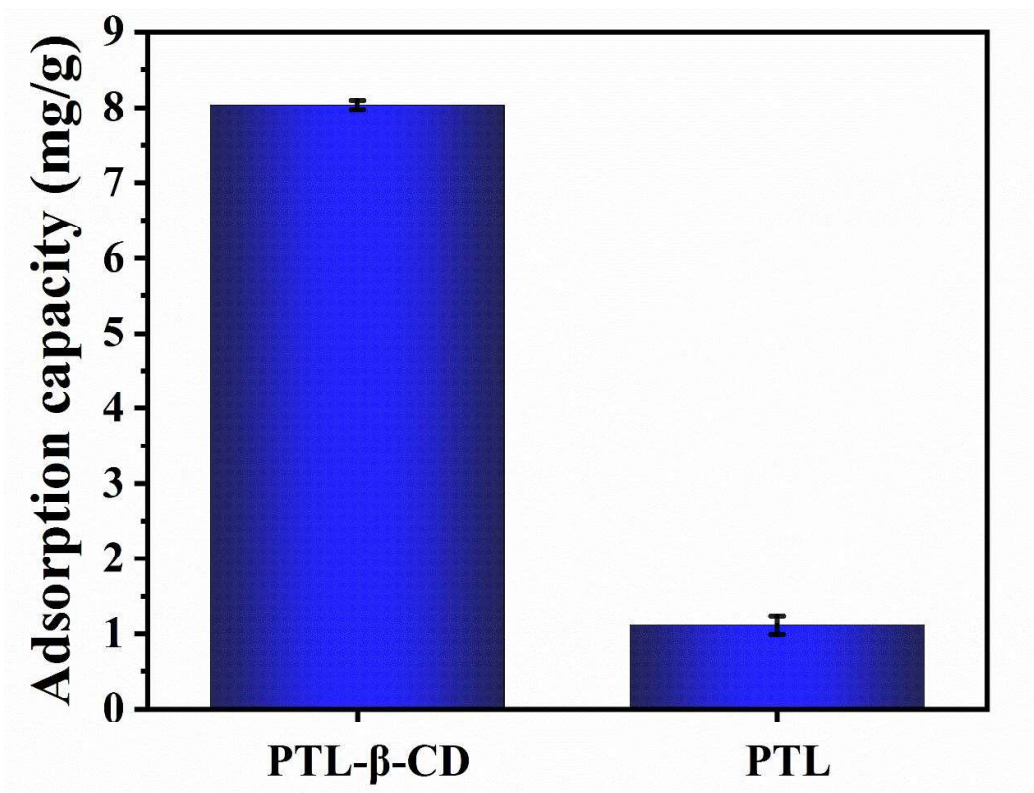


**Figure S10.** Adsorption capacity of uranium ions by PTL-β-CD and PTL.

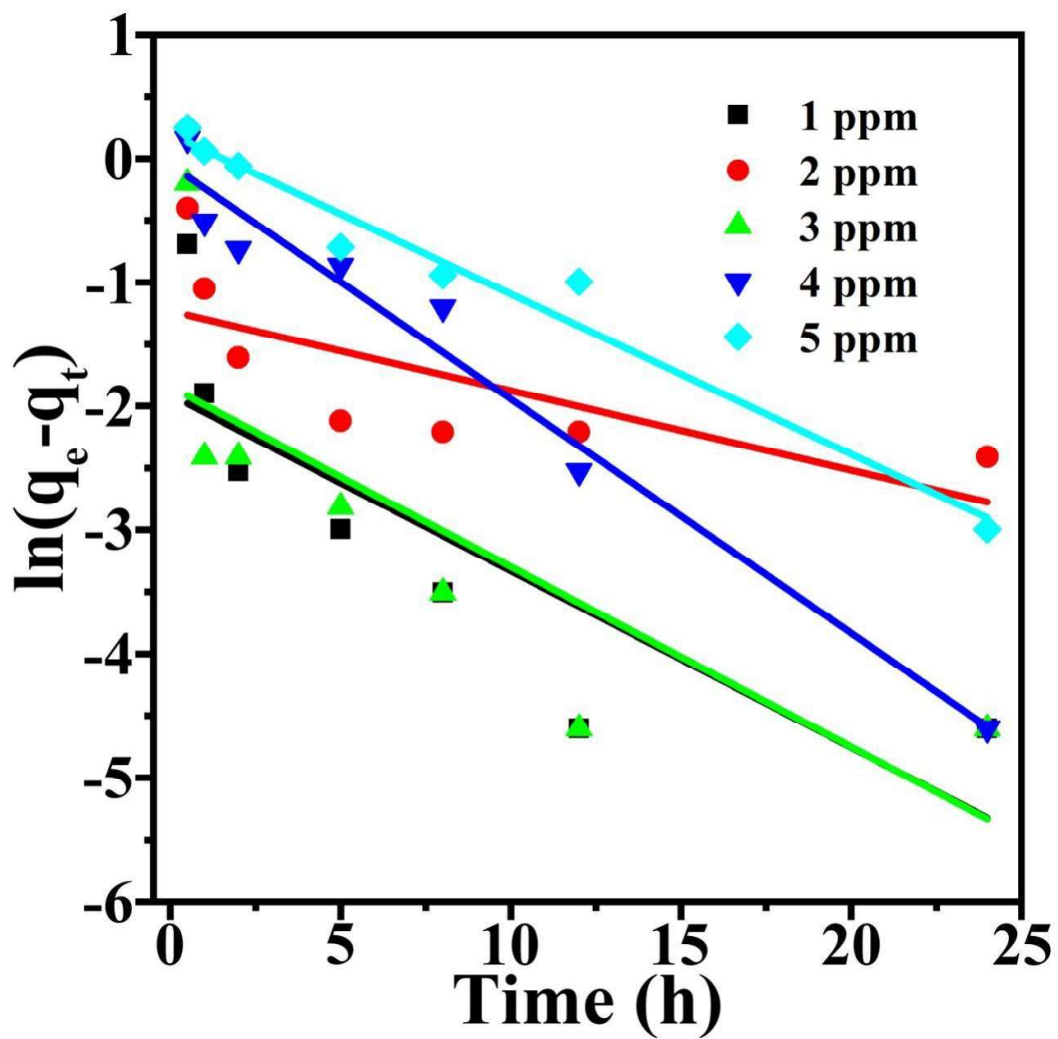


**Figure S11.** Pseudo-first-order kinetic fitting for the adsorption of uranium ions on the PTL-β-CD.

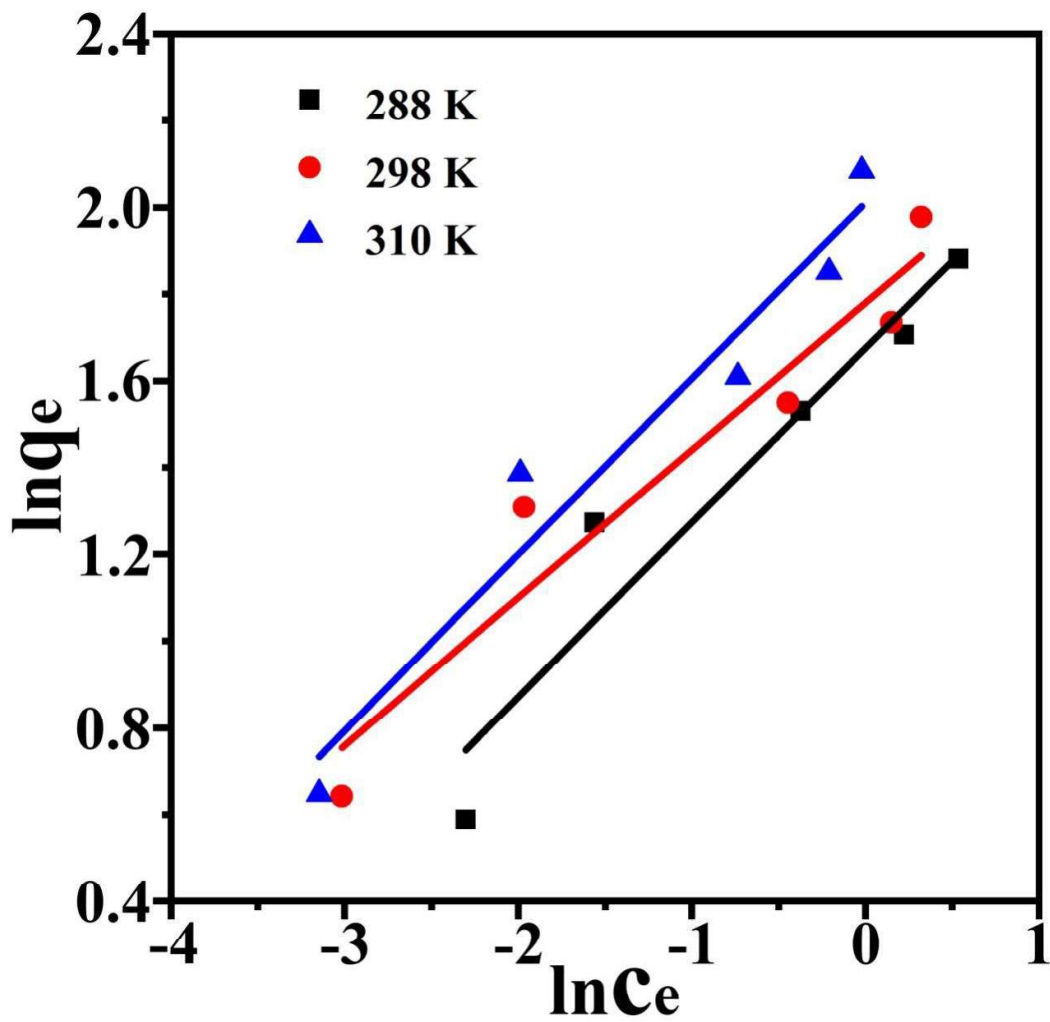
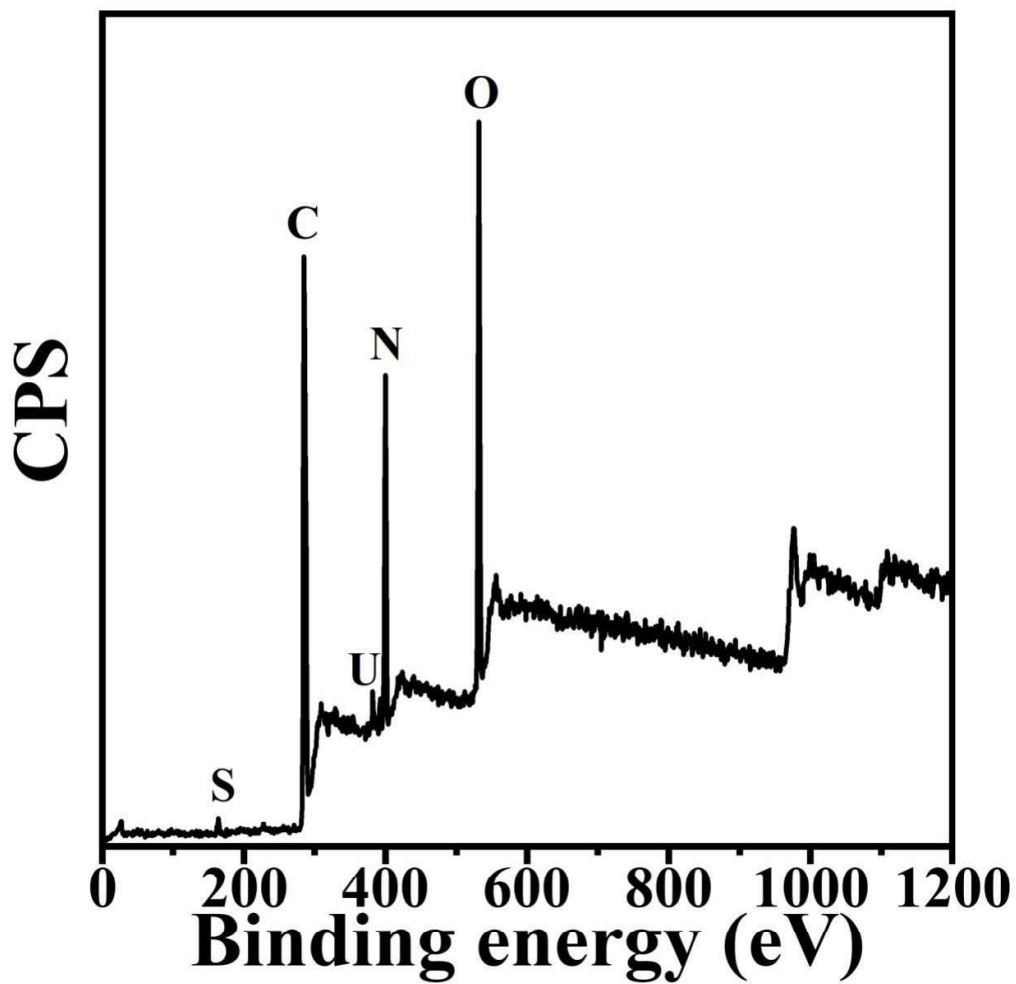


Figure S12. Freundlich isotherm fitting for the adsorption of uranium ions on the PTL- $\beta$ -CD.



**Figure S13.** XPS spectrum of the PTL- $\beta$ -CD after the uranium ions adsorption.

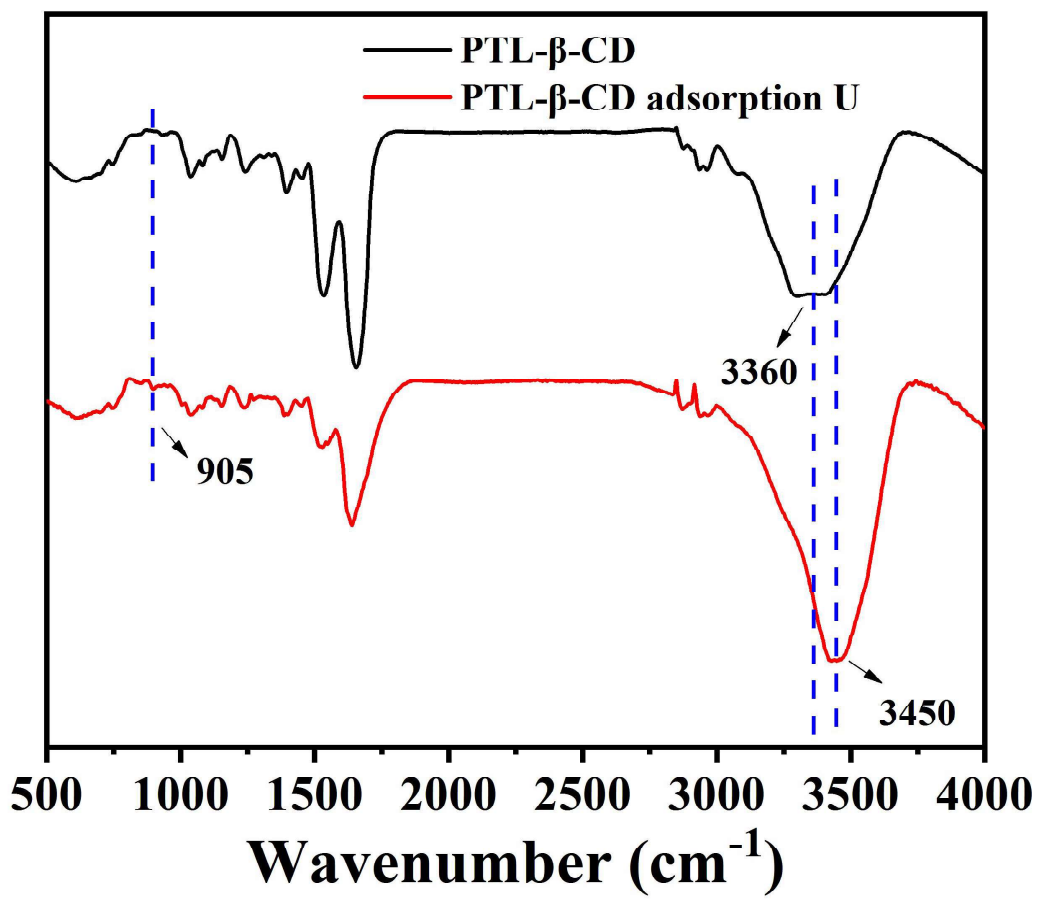
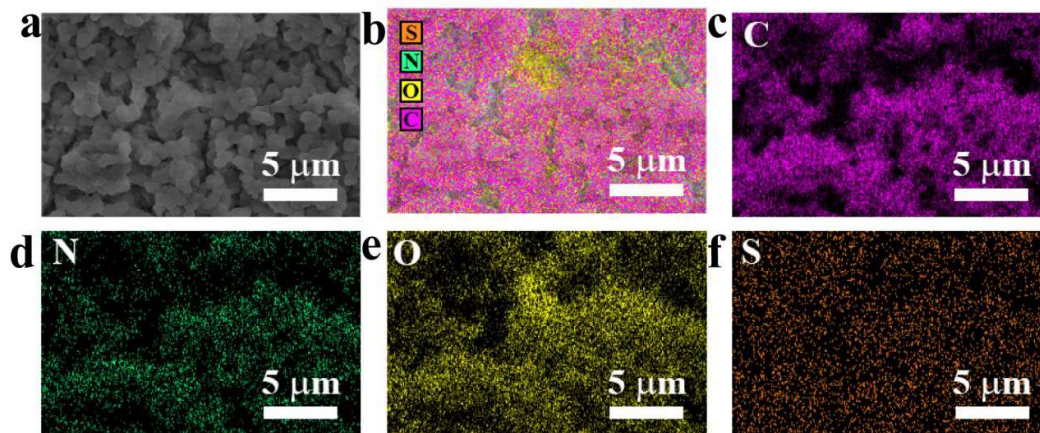
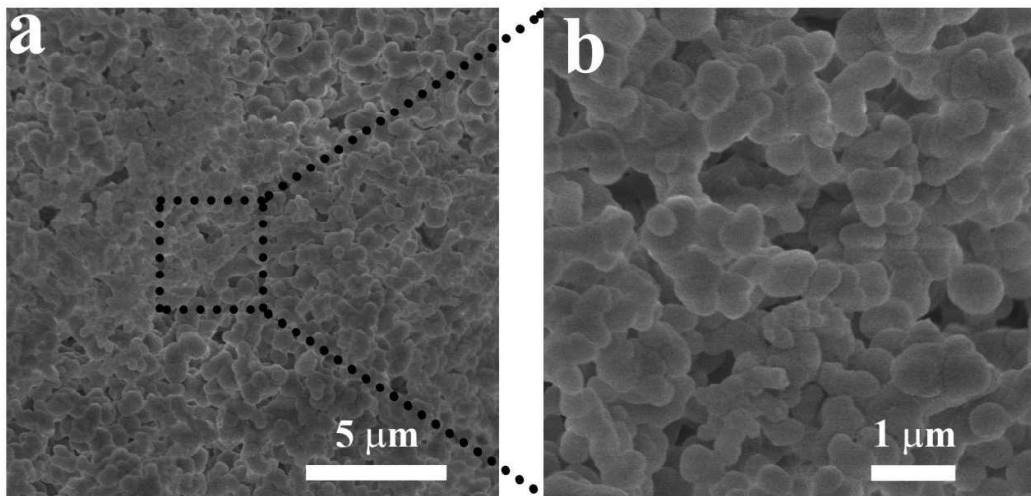


Figure S14. FTIR spectra of the PTL-β-CD before and after the uranium ions adsorption.



**Figure S15.** SEM images and its elemental distribution maps of C, N, O, S of the PTL-β-CD.



**Figure S16.** SEM images of the PTL-β-CD after adsorption of uranium ions.

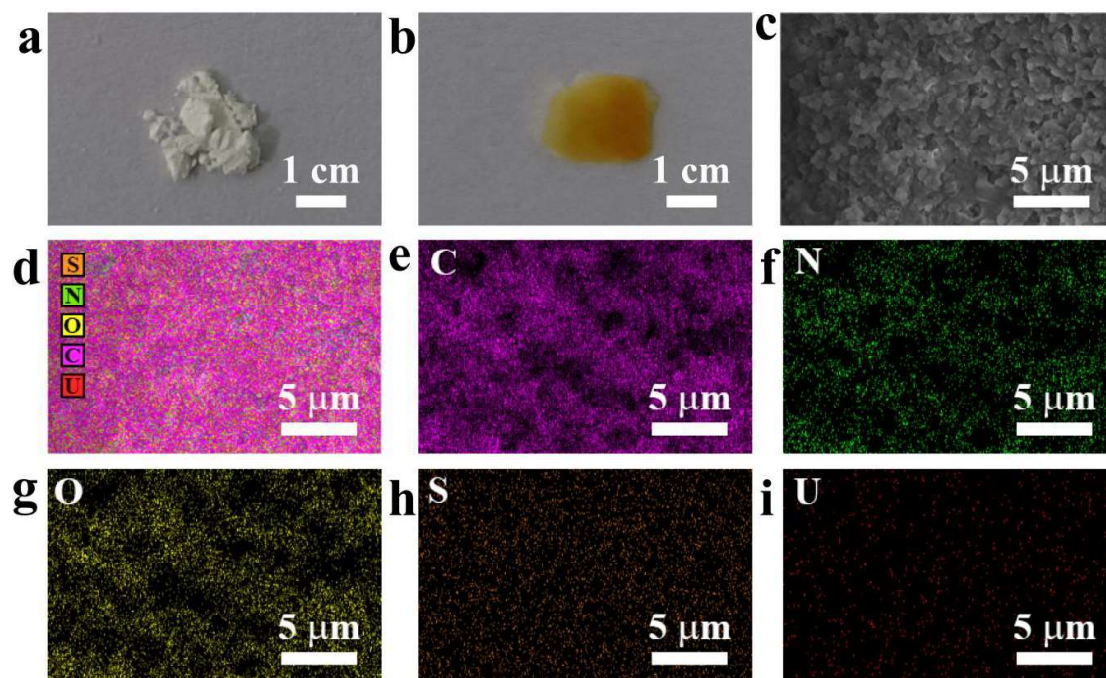


**Figure S17.** Photographs of the PTL-β-CD aggregates before (a) and after (b) adsorbing uranium ions. SEM images (c) and its elemental distribution maps of C, N, O, S, U (e-i) of the PTL-β-CD aggregates after uranium ions adsorption.



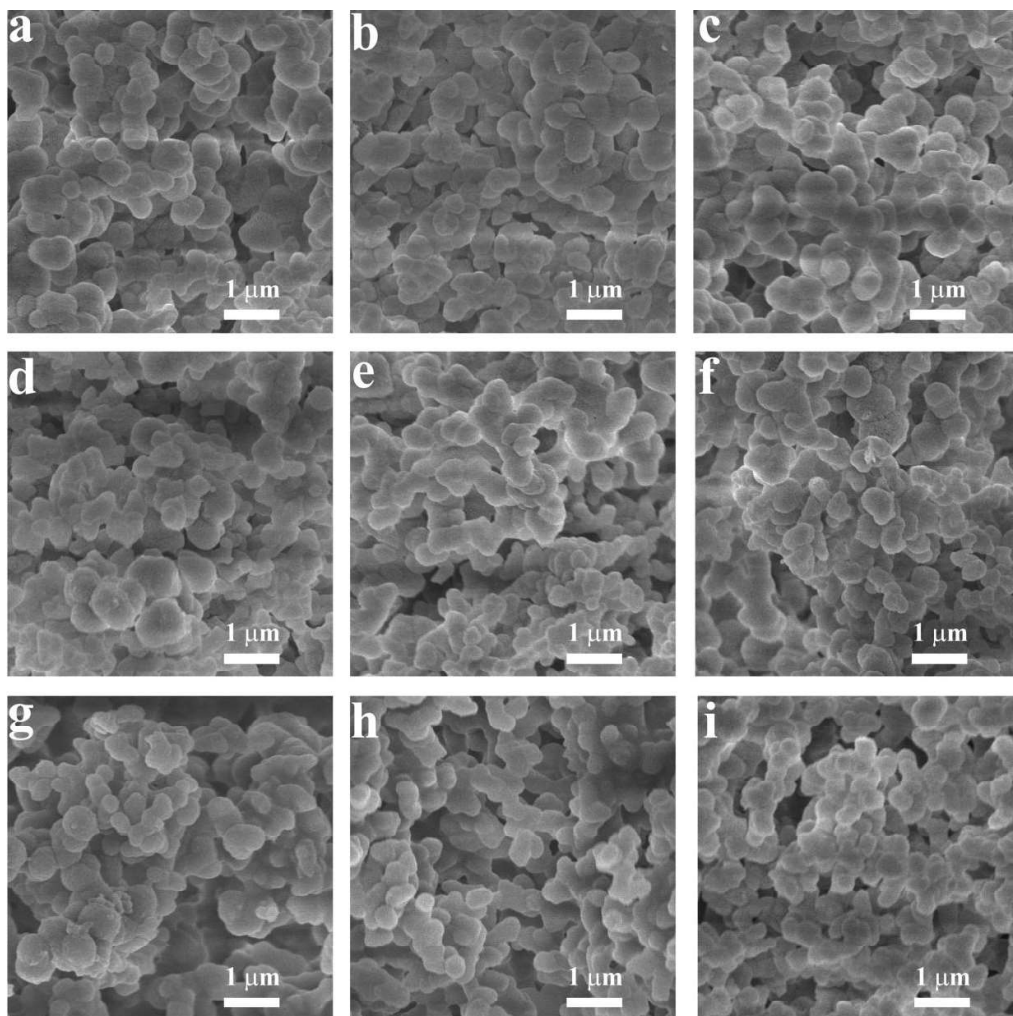


**Figure S18.** SEM images showing the morphology of the PTL- $\beta$ -CD after the treatment under various extreme conditions (a, ultrasonic for 3 min; b, petroleum ether for 2 h; c, dichloromethane for 2 h; d, ethyl acetate for 2 h; e, tetrahydrofuran for 2 h; f, hexane for 2 h; g, ethanol for 2 h; h, pH 2 for 2 h; i, pH 12 for 2 h).

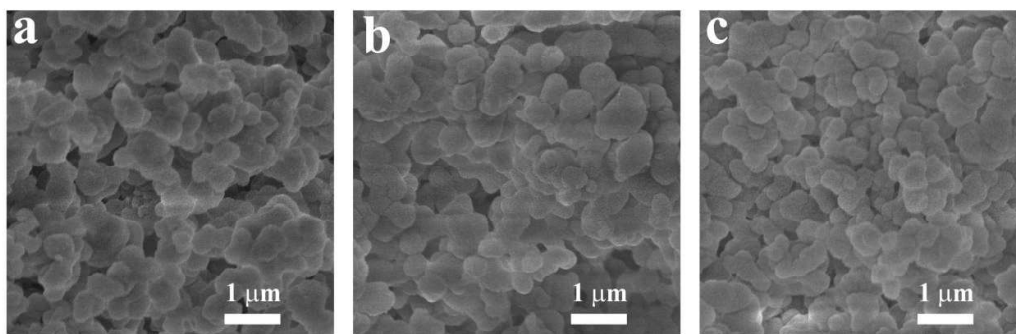


**Figure S19.** SEM images showing the morphology of the PTL- $\beta$ -CD after three adsorption-desorption cycles (a), five adsorption-desorption cycles (b), ten adsorption-desorption cycles (c), respectively.

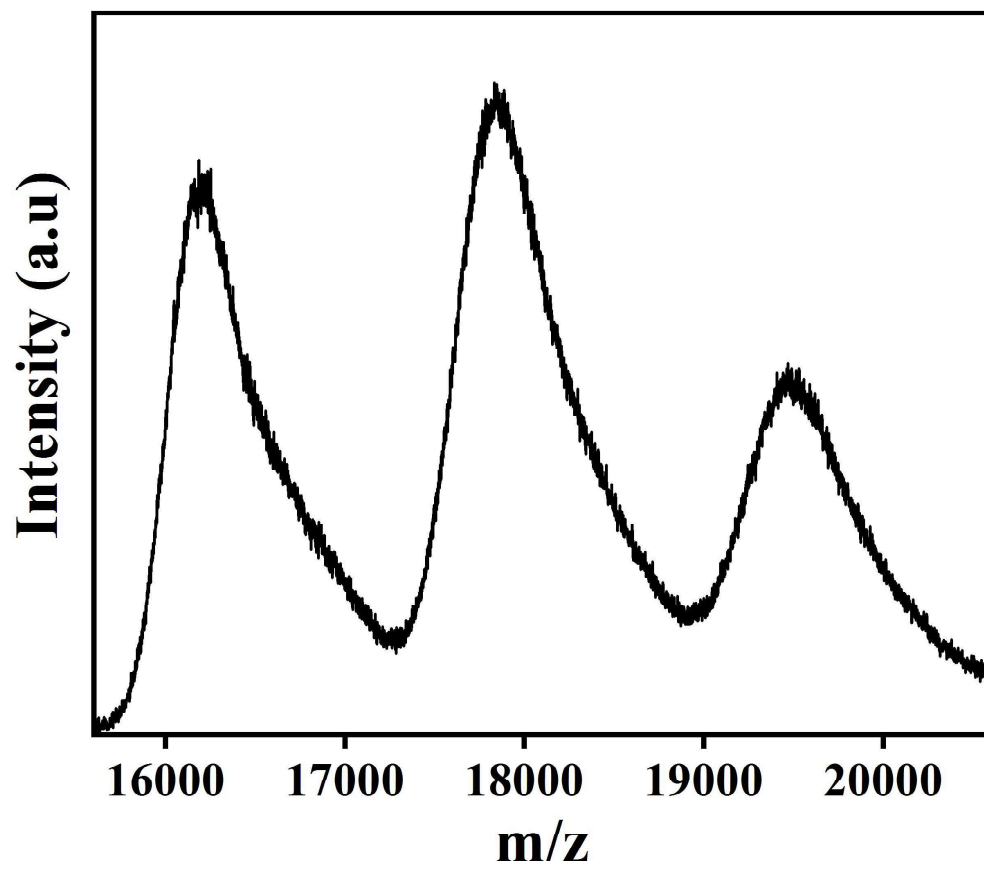


**Figure S20.** The molecular weight of PTL- $\beta$ -CD after uranium ions desorption.

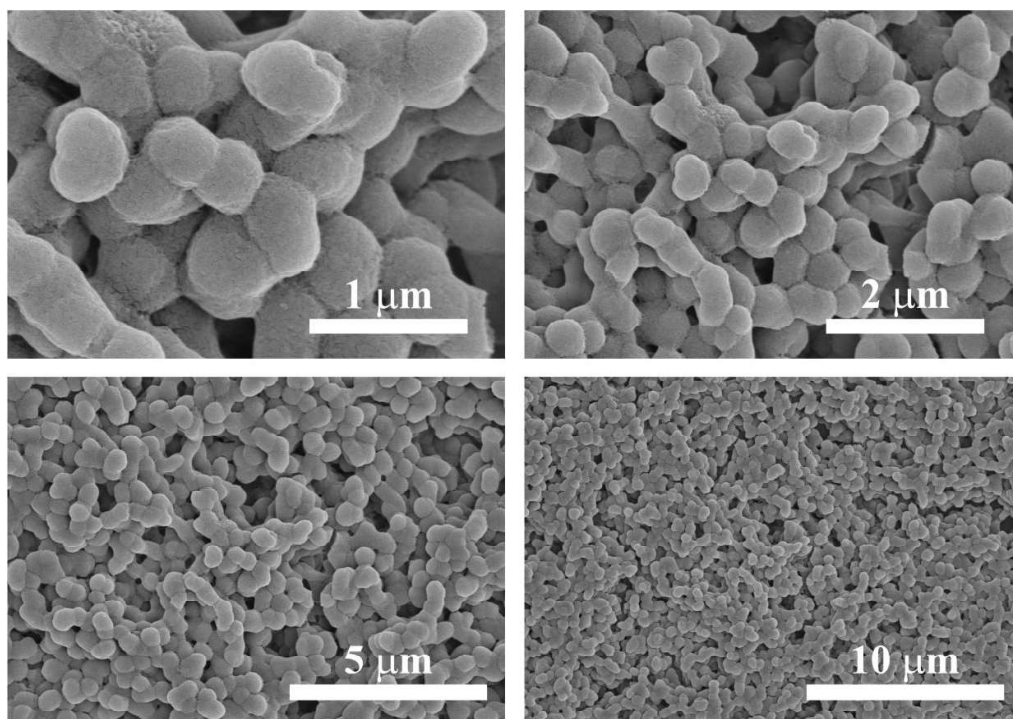


**Figure S21.** SEM images of the PTL- $\beta$ -CD aggregates after immersed in simulated sea water for 30 days.

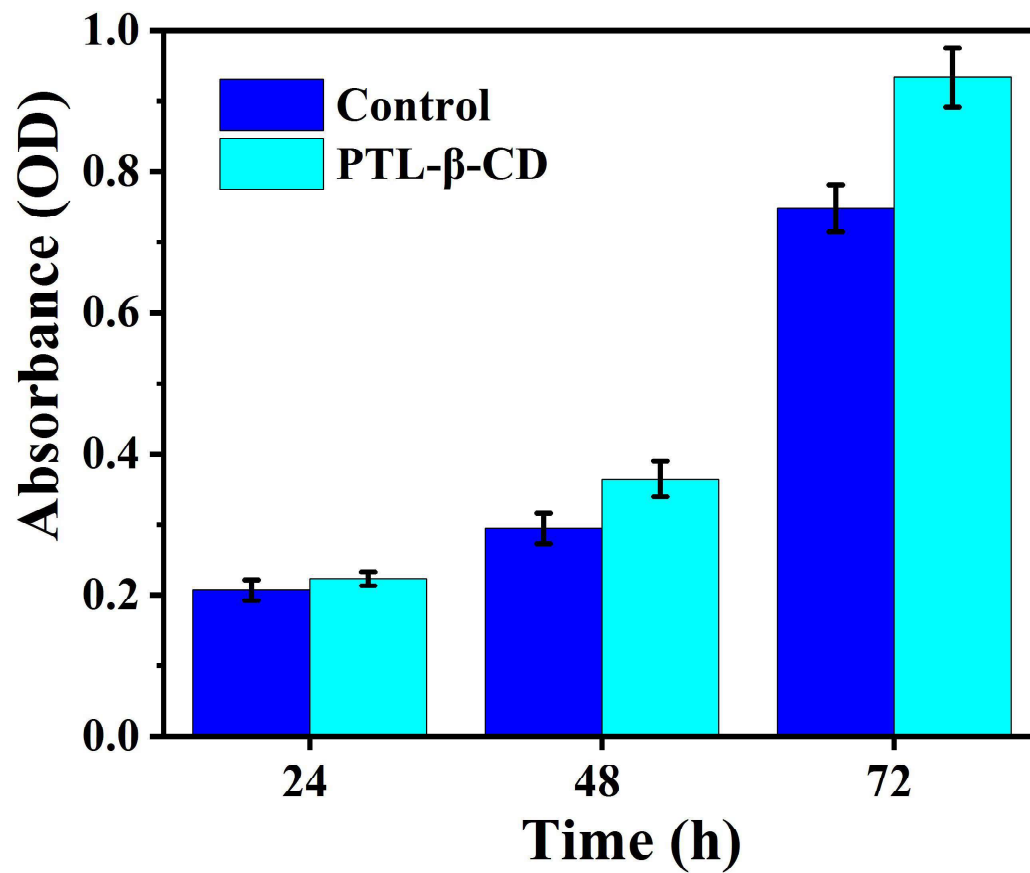


**Figure S22.** After culturing for 24, 48 and 72 hours, the OD value of 3T3 cells culture solution.

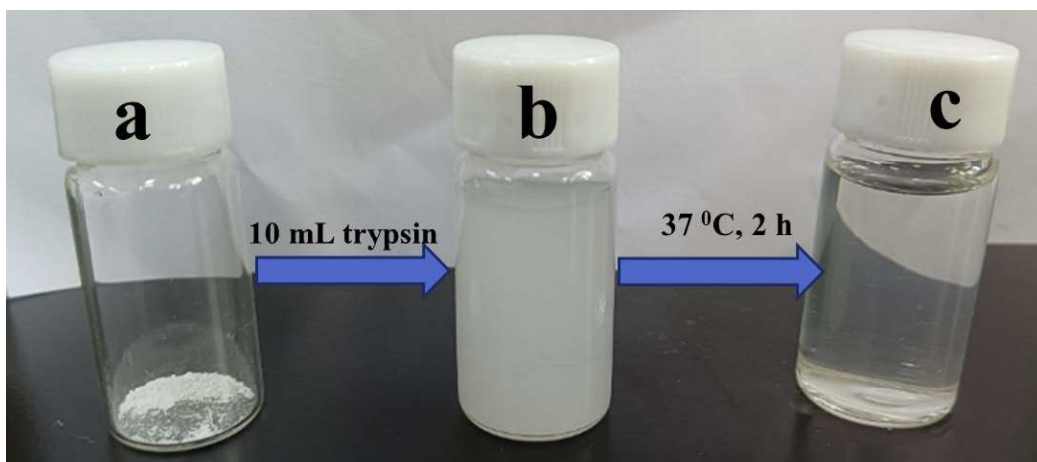


**Figure S23.** Degradation process of the PTL-β-CD aggregates by trypsin.

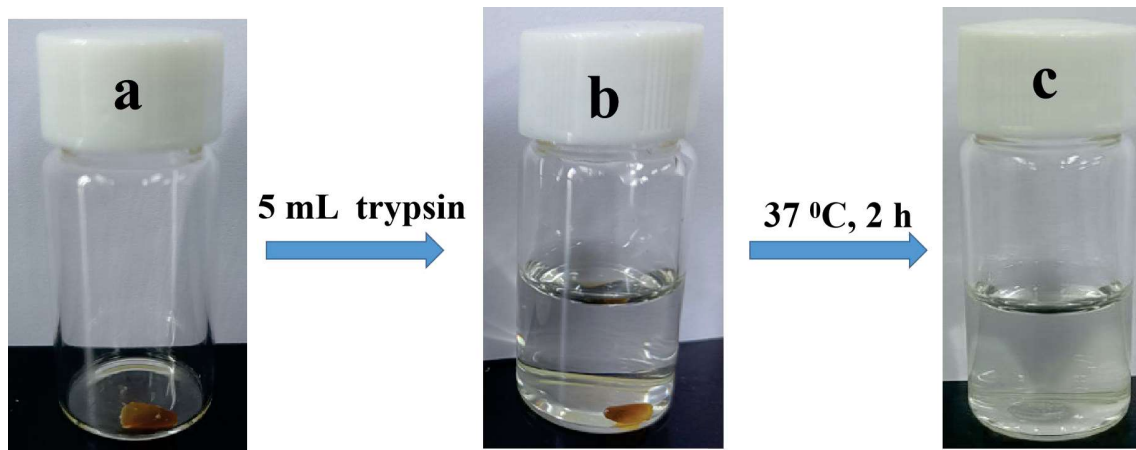


**Figure S24.** Degradation process of the PTL- $\beta$ -CD aggregates (after adsorption of uranium ions) by trypsin.

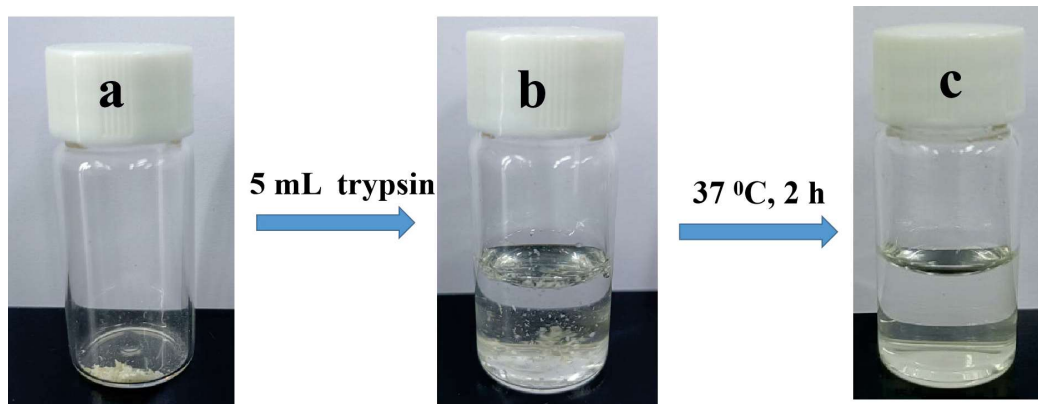


**Figure S25.** Degradation process of the PTL- $\beta$ -CD aggregates (after desorption of uranium ions) by trypsin.



**Supporting Tables:****Table S1.** A comparison of pseudo-first-order and pseudo-second-order fitting for the experimental data.

Adsorbents	$c_0$ ppm	$q_e$ (exp)	Pseudo-first-order		Pseudo-second-order		
			$k_1$	$R_1^2$	$k_2$	$q_e$	$R_2^2$
			$h^{-1}$		g/(mg.h)	mg/g	
PTL- $\beta$ -CD	1	1.81	0.1074	0.6207	0.5555	1.80	0.9999
	2	3.52	0.1067	0.8047	0.2859	3.50	0.9999
	3	4.65	0.1127	0.9391	0.2164	4.62	0.9997
	4	5.60	0.0854	0.8680	0.1821	5.49	0.9998
	5	6.60	0.1042	0.9612	0.1543	6.48	0.9977

**Table S2.** Langmuir and Freundlich isotherm adsorption parameters for the adsorption of uranium ions on the PTL- $\beta$ -CD at different temperatures.

	T/K	Langmuir constants			$R_L$	Freundlich constants		
		$q_m$ (mg/g)	$k_L$ (L/mg)	$R_L^2$		$k_F$	$1/n$	$R_F^2$
PTL- $\beta$ -CD	288	9.50	0.0077	0.9960	0.8665-0.9923	4.78	0.29	0.9046
	298	11.27	0.0056	0.9950	0.8992-0.9944	5.56	0.29	0.9536
	310	12.21	0.0032	0.9986	0.9398-0.9968	6.42	0.31	0.9251

**Table S3.** Thermodynamic parameters for the adsorption of uranium ion onto the PTL- $\beta$ -CD.

$c_0$ (ppm)	$\Delta H^0$ (kJ $\cdot$ mol $^{-1}$ )	$\Delta G^0$ (kJ mol $^{-1}$ )			$\Delta S^0$ (J $\cdot$ mol $^{-1}$ $\cdot$ k $^{-1}$ )
		288 K	298 K	310 K	
1	29.57	-5.26	-7.34	-7.99	122.02
2	15.12	-5.13	-6.41	-6.72	71.02
3	15.51	-2.89	-3.23	-4.27	63.54
4	20.12	-1.88	-2.21	-3.53	75.92
5	26.57	-1.56	-2.39	-3.70	97.54

**Table S4.** Element content before and after adsorption of uranium ion by PTL- $\beta$ -CD.

Element	wt.% (before)	wt.% (after)
C	51.8	52.4
O	29.0	26.6
N	17.4	19.4
S	1.8	1.1
U	0	0.5

**Table S5.** The uranium ion adsorption capacity per unit area of different adsorbents.

Adsorbents	Adsorption capacity per unit area ( $\text{mg}\cdot\text{g}^{-1}\cdot\text{m}^{-2}$ )	Reference
Resin	0.015	1
Activated carbon	0.029	2
MOF	0.160	3
COF	0.477	4
Active biochar	0.421	5
UiO-66	0.304	6
Biocomposite adsorbent	0.18	7
Mesoporous silica	0.279	8
Aromatic frameworks	0.204	9
Polymeric peptide	0.396	10
Nanofibrous	0.038	11
BP@CNF-MOF	0.872	12
DSHM-DAMN	0.371	13
$\beta$ -CD/Graphene	0.691	14
MWCNTs-CDP	0.502	15
PTL- $\beta$ -CD	1.405	this work

## Reference

- [1] J. Bai, X. Ma, C. Gong, et al, *J. Mol. Liq.*, 2020, **320**, 114443.
- [2] A. Mellah, S. Chegrouche, M. Barkat, *J. Colloid Interface Sci.*, 2006, **296**, 434-441.
- [3] M. Carboni, C. W. Abney, S. Liu, et al, *Chem. Sci.*, 2013, **4**, 2396-2402.
- [4] Q. Sun, B. Aguila, L. D. Earl, et al, *Adv. Mater.*, 2018, **30**, 1705479.
- [5] Q. Zhang, Y. Wang, Z. Wang, et al, *J. Alloys Compd.*, 2021, **852**, 156993.
- [6] Q. Yu, Y. Yuan, J. Wen, et al, *Adv. Sci.*, 2019, **6**, 1900002.
- [7] S. Aytas, D. A. Turkozu, C. Gok, *Desalination*, 2011, **280**, 354-362.
- [8] S. Yang, J. Qian, L. Kuang, et al, *ACS Appl. Mater. Interfaces*, 2017, **9**, 29337-29344.
- [9] Y. Yuan, Y. Yang, X. Ma, et al. *Adv. Mater.*, 2018, **30**, 1706507.
- [10] Y. Yuan, Q. Yu, M. Cao, et al, *Nat. Sustain.*, 2021, **4**, 708–714.
- [11] S. Xie, X. Liu, B. Zhang, et al, *J. Mater. Chem. A*, 2015, **3**, 2552-2558.
- [12] M. Chen, T. Liu, X. Zhang, et al, *Adv. Funct. Mater.*, 2021, 2100106.
- [13] J. Zhang, H. Zhang, Q. Liu, et al, *Chem. Eur. J.* 2019, **368**, 951-958.
- [14] N. Li, L. Yang, D. Wang, et al, *Environ. Sci. Technol.*, 2021, **55**, 9181-9188.
- [15] J. Xue, H. Zhang, D. Ding, et al, *Ind. Eng. Chem. Res.* 2019, **58**, 4074-4083.